Mathematical Morphology:
The Hamilton-Jacobi Connection

A. B. Arehart
Brown University
Providence, RI 02912

L. Vincent
Xerox Imaging Systems
Peabody, MA 01960

B. B. Kimia
Brown University
kimia@lems.brown.edu

Abstract

In this paper we complement the standard algebraic view of mathematical morphology with a geometric, differential view. Three observations underlie this approach: 1) certain structuring elements (convex) are scalable in that a sequence of repeated operations is equivalent to a single operation, but with a larger structuring element of the same shape; 2) to determine the outcome of the operation, it is sufficient to consider how the boundary is modified; 3) the modifications of the boundary are such that we can move each point along the normal by a certain amount, which is dependent on the structuring element. Taken together, these observations, when the size of the structuring element shrinks to zero, assert that mathematical morphology operations with a convex structuring element are captured by a differential deformation of the boundary along the normal, governed by a Hamilton-Jacobi partial differential equation (PDE). A second theme of this paper is to show that mathematical morphology operations can be numerically implemented in a highly accurate fashion as the solution of these PDEs.

Introduction In this paper we complement the standard algebraic view of mathematical morphology with a geometric differential view. Classically, mathematical morphology treats binary images as sets and grayscale images as functions and operates on them in the spatial domain via *morphological transformations*, using *structuring elements* [17, 27, 5, 28]. While there is a growing interest in applying mathematical morphology to abstract spaces such as lattices [28, 6], graphs [29] or manifolds [20], our interest lies in considering geometric interpretations of morphological transformations; see also [2, 4, 25]. We restrain ourselves to the Euclidean plane and consider the morphological operators $\psi : \mathbb{R}^2 \longrightarrow \mathbb{R}^2$ transforming a set (shape) into another set. In this framework, we formulate basic morphological operators as partial differential equations governing the geometric evolution of the shape.

To illustrate our approach consider the dilation transformation of a shape with a disk structuring element. The transformed shape is the union of all disks centered on points of the original shape. The boundary of the transformed shape is a curve parallel to the boundary of the original shape with a distance equal to the radius of the disk. This is precisely Huygens' principle for wavefront propagation [7, 10], relating operations on algebraic constructs, *i.e.*, sets of points and operations on geometric entities, *i.e.*, curves representing the boundary. We will now show that this is true for all convex structuring elements, by studying morphological operations in a shape evolution framework.

The geometric evolution of shapes was extensively studied by Kimia *et.al.* [9, 13]. Their "shape from deformation" framework captures the essence of shape through the deformations of it which were shown to be modeled geometrically as follows: Consider a shape represented by the curve $\mathcal{C}_0(s) = (x_0(s), y_0(s))$ undergoing a deformation, where s is the parameter along the curve (not necessarily the arclength), x_0 and y_0 are the Cartesian coordinates and the subscript $_0$ denotes the initial curve prior to deformation. Now, let each point of this curve move by some arbitrary amount in some arbitrary direction; see Figure 1. It can be shown that all deformations reduce to an equivalent deformation along the normal described by

$$\begin{cases} \frac{\partial \mathcal{C}}{\partial t} & = \beta(s,t)\vec{N} \\ \mathcal{C}(s,0) & = \mathcal{C}_0(s), \end{cases} \quad (1)$$

Observe that when $\beta(s,t) = 1$, the evolution describes unit movement along the normal which, through an application of Huygens' principle, is equivalent to the morphological operation of dilation with a circular structuring element. Similarly, $\beta(s,t) = -1$, corresponds to erosion with a circular structuring element. It is therefore reasonable that alternate forms of β, should correspond to interesting morphology operations, as we will show in this paper. For a review of mathematical morphology see [1], and [17, 27, 5, 28].

Mathematical Morphology and Geometric Evolution The *geometric* view of the *algebraic* operations of mathematical morphology, is founded on three observations. First, observe that for a class of convex structuring elements $\mathcal{\hat{B}}$, n repeated dilations (or erosions) with a structuring element $\mathcal{B} \in \mathcal{\hat{B}}$, is equivalent to a single dilation with a structuring element of the same shape, but which is "scaled up" n times. Let us denote a structuring element scaled by λ as $\mathcal{B}(\lambda)$. For example, 10 dilations with a circle of radius of 1, $\mathcal{B}(1)$, is exactly a single dilation with a
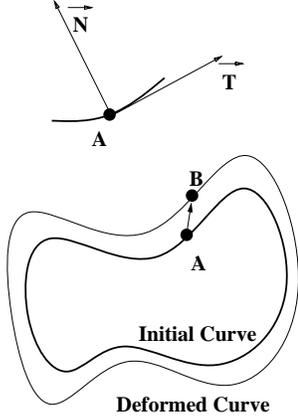
Figure 1: The points on the initial curve A move to B to generate a new curve. The direction and magnitude of this motion is arbitrary in order to capture general deformations.

circle of radius 10, $\mathcal{B}(10)$. The class of structuring elements $\hat{\mathcal{B}}$ for which this property holds is exactly the set of *convex* structuring elements [17, Theorem 1.5.1, pp. 22–23]. Now, conversely, given a single operation with a convex structuring element, the operation can be decomposed as a sequence of n operations with the same structuring element but of "size" $1/n^{\mathrm{th}}$ the original. In the limit, as $n \to \infty$, this notion of size constitutes the "time" axis for the differential deformation.

Second, observe that the outcome of mathematical morphology operations with a shape $\mathcal{S}$, can be determined solely from its boundary, $\partial \mathcal{S}$ [29]. Thus, the mapping form the shape $\mathcal{S}$ to $\mathcal{S}'$ by morphological operations can be reduced to operations taking $\partial \mathcal{S}$ to $\partial \mathcal{S}'$. As such, appropriate geometric evolution of the boundary can model algebraic mathematical morphology operations on shapes as sets.

Third, we now show that for a sufficiently small but finite structuring element, mathematical morphology operations along the smooth portions of the boundary can be viewed as a deformation along the normal by a certain amount, Figure 1. Formally, let some shape $\mathcal{C}(s,t)$ evolve by a mathematical morphology operation, say dilation, by some structuring element $\mathcal{B}(\lambda)$ of size λ, to a new shape $\mathcal{C}(s, t+\lambda)$. This evolution can be represented as

$$\mathcal{C}(s, t+\lambda) - \mathcal{C}(s,t) = {}, (s,t,\lambda)\vec{N}(s,t), \qquad (2)$$

where $,$ is the distance along $\vec{N}$ that a point on the boundary moves in a dilation operation with a structuring element of size λ. Since $, (s,t,0) = 0$, using (2) in the limiting case as $\lambda \to 0$,

$$\frac{\partial \mathcal{C}}{\partial t} = \lim_{\lambda \to 0} \frac{, (s,t,\lambda)}{\lambda}\vec{N} = \frac{\partial , (s,t,0)}{\partial \lambda}\vec{N}. \qquad (3)$$

Therefore, the mathematical morphology operation of dilation with a structuring element of size t is governed by the partial differential equation

$$\begin{cases} \frac{\partial \mathcal{C}}{\partial t} & = \beta(s,t)\vec{N} \\ \mathcal{C}(s, 0) & = \mathcal{C}_0(s), \end{cases} \qquad (4)$$

where $\beta(s,t) = \frac{\partial \Gamma(s,t,0)}{\partial \lambda}$, and $\mathcal{C}_0(s)$ is the boundary of the original shape. Note that at singular points, the deformation is handled by notions of weak solution, shock, rarefaction wave, and entropy in the context of the "shape from deformation" framework, as introduced in [8, 9, 13].

Morphological Evolution is Independent of Original Shape In the above model, β depends on the structuring element and the original shape. Since the boundary of the transformed shape is the union of all structuring elements centered on the boundary of the original shape, the amount of deformation along the normal β, is the maximum deformation implied by each. For a finite size arbitrary structuring element, the maximal deformation may (and often is) attained by a structuring element that is not centered at the point to be deformed. This points to the possibility that the maximal deformation may depend on the local shape, *e.g.*, curvature, of the original set. It is intriguing, however, this is not the case and in fact β, the amount that each point moves out along the normal, does not depend on the "shape" of the original set, but rather only on the its orientation:

Theorem 1 *The amount of differential deformation, β, of a shape $\mathcal{S}$ at a point P due to dilation (erosion) with a convex structuring element $\mathcal{B}$, is the maximal (minimal) projection of $\mathcal{B}$ onto the normal $\vec{N}$ of the boundary at P.*

Corollary 1 *The differential deformation, β, at a point P of the boundary, does not depend on f, the function representing the local boundary of the shape $\mathcal{S}$ at P.*

Proof: For simplicity, and without loss of generality, we consider dilations; by duality, the approach also applies to erosions. Let $\mathcal{S}$ be an arbitrary shape being operated on by a structuring element $\mathcal{B}$. We will derive the deformation β at an arbitrary point P on the boundary. Consider the local coordinate system formed by the tangent $\vec{T}$ and normal $\vec{N}$ at P and represent the shape $\mathcal{S}$ locally in this coordinate system as $(\omega, f(\omega))$, Figure 2. Note that by construction, $f(0) = 0$ and $f'(0) = 0$. To determine β, we will move the center of the structuring element $\mathcal{B}$ over the boundary (which is parametrized by ω), determine the intersection of $\mathcal{B}$ with the normal, $\gamma(\omega, \lambda)$, determine the maximum deformation over all ω, $, (\lambda)$, and then take the limit as the size of the structuring element $\lambda \to 0$. It is important to emphasize that when the structuring element has finite size, the maximal intersection $, (\lambda)$ is not necessarily attained when the

structuring element is centered at the point of deformation, P. However, we now prove that *differentially* the deformation is attained by the maximal projection of $\mathcal{B}$ centered at P.

Denote the graph of the *unit* structuring element in $(\vec{T}, \vec{N})$ as $(\xi, h(\xi))$, where $\xi_{\min} \leq \xi \leq \xi_{\max}$. The *scaled* structuring element at scale λ is then described by $(\xi, \lambda h(\frac{\xi}{\lambda}))$, where $\lambda \xi_{\min} \leq \xi \leq \lambda \xi_{\max}$. To find the intersection of $\mathcal{B}$ centered at $(\omega, f(\omega))$, and the normal $\vec{N}$, denoted by $\gamma(\omega, \lambda)$, we solve for η in the following

$$
\begin{cases}
\eta - f(\omega) & = \lambda h(\frac{\xi - \omega}{\lambda}) \qquad \lambda\xi_{\min} \leq \xi - \omega \leq \lambda\xi_{\max} \\
\xi & = 0,
\end{cases}
\tag{5}
$$

so that

$$
\gamma(\omega, \lambda) = f(\omega) + \lambda h(\frac{-\omega}{\lambda}).
\tag{6}
$$

By definition, $,(\lambda)$ is the maximum of γ over ω, where the point of maximum is denoted by $\Omega(\lambda) = \omega_{\max}(\lambda)$. To ensure that Ω gives a maximum of γ,

$$
\begin{cases}
\frac{\partial \gamma(\Omega)}{\partial \omega} & = f'(\Omega) - h'(\frac{-\Omega}{\lambda}) = 0. \\
\frac{\partial^2 \gamma(\Omega)}{\partial \omega^2} & = f''(\Omega) + \frac{1}{\lambda} h''(\frac{-\Omega}{\lambda}) < 0.
\end{cases}
\tag{7}
$$

The latter is guaranteed for small enough λ by convexity of the structuring element $h''(\xi) < 0$. Rather than solving for Ω, recall that we seek β, the amount of differential deformation, where

$$
\beta = \lim_{\lambda \to 0} \frac{\partial ,}{\partial \lambda},
\tag{8}
$$

$$
,(\lambda) = f(\Omega(\lambda)) + \lambda h(\frac{-\Omega(\lambda)}{\lambda}),
\tag{9}
$$

and where Ω is determined from (7) as

$$
f'(\Omega) - h'(\frac{-\Omega}{\lambda}) = 0.
\tag{10}
$$

Note that

$$
\begin{aligned}
\frac{\partial \Gamma}{\partial \lambda} & = f'(\Omega)\Omega_\lambda + h(\frac{-\Omega}{\lambda}) + h'(\frac{-\Omega}{\lambda})[-\Omega_\lambda + \frac{\Omega}{\lambda}] \\
& = [f'(\Omega) - h'(\frac{-\Omega}{\lambda})]\Omega_\lambda + h(\frac{-\Omega}{\lambda}) + h'(\frac{-\Omega}{\lambda})\frac{\Omega}{\lambda} \\
& = h(\frac{-\Omega}{\lambda}) + h'(\frac{-\Omega}{\lambda})\frac{\Omega}{\lambda},
\end{aligned}
\tag{11}
$$

so that

$$
\beta = \lim_{\lambda \to 0} \left(h(\frac{-\Omega}{\lambda}) + h'(\frac{-\Omega}{\lambda})\frac{\Omega}{\lambda} \right).
\tag{12}
$$

Observe that since Ω depends on f, (10), then it would seem that β is also dependent on the shape of the original set, f. However,

$$
\begin{cases}
\lim_{\lambda \to 0} \Omega = 0 \\
\lim_{\lambda \to 0} f'(\Omega) = f'(0) = 0,
\end{cases}
\tag{13}
$$

together with (10) implies that

$$
\lim_{\lambda \to 0} h'(\frac{-\Omega}{\lambda}) = 0,
\tag{14}
$$

leading to the observation that

$$
\beta = \lim_{\lambda \to 0} h(\frac{-\Omega}{\lambda}) = h(\lim_{\lambda \to 0} \frac{-\Omega}{\lambda}).
\tag{15}
$$

Since we are only interested in β, let $x_0 = \lim_{\lambda \to 0}(\frac{-\Omega}{\lambda})$ and rewrite (15) and (14) as

$$
\begin{cases}
\beta & = h(x_0) \\
h'(x_0) & = 0.
\end{cases}
\tag{16}
$$

Stated differently, to obtain β at a point P, find the maximal projection of the structuring element, represented by h onto the normal $\vec{N}$. ∎

While in the above theorem it was assumed that h is differentiable, the theorem also holds for a piecewise smooth function, h.

Examples of β Theorem 1 allows us to determine β and then numerically simulate the differential equation. Since the projection of a circle is its radius, then $\beta = 1$ for a circle, as we have seen before. A more interesting example is an ellipse; it is not difficult to show the following lemma [1]:

Lemma 1 *Consider an ellipse structuring element $\mathcal{B}$, with major and minor axes $(2A, 2B)$, and orientation $\theta_\mathcal{B}$ (i.e., the angle between its major axis and the x-axis is $\theta_\mathcal{B}$). Then dilations with $\mathcal{B}$ are equivalent to*

$$
\begin{cases}
\frac{\partial \mathcal{C}}{\partial t} & = \beta(\theta(s, t))\vec{N} \\
\mathcal{C}(s, 0) & = \mathcal{C}_0(s),
\end{cases}
\tag{17}
$$

where $\theta = \angle(\vec{T}, x\text{-axis})$ and

$$
\beta(\theta) = \sqrt{A^2 \sin^2(\theta - \theta_\mathcal{B}) + B^2 \cos^2(\theta - \theta_\mathcal{B})}.
\tag{18}
$$

Similarly, it is not difficult to obtain β for other structuring elements, *e.g.*, square, diamond, rectangle, *etc*, [1].

The Hamilton-Jacobi Connection Thusfar, we have shown that mathematical morphology operations can be modeled as geometric evolution governed by a partial differential equation as in (4), where β is a function of the orientation of the boundary, $\theta = \angle(\vec{T}, x\text{-axis})$. Unfortunately, direct simulations of equation (4) are not robust! Observe that shapes undergoing morphological operations change their topology in that they merge and split, leading to problems in administrating newly formed boundaries and annihilated ones. In addition, as shapes evolve, some boundary points bunch-up and merge to form singularities, leading to numerical errors. Typically, a
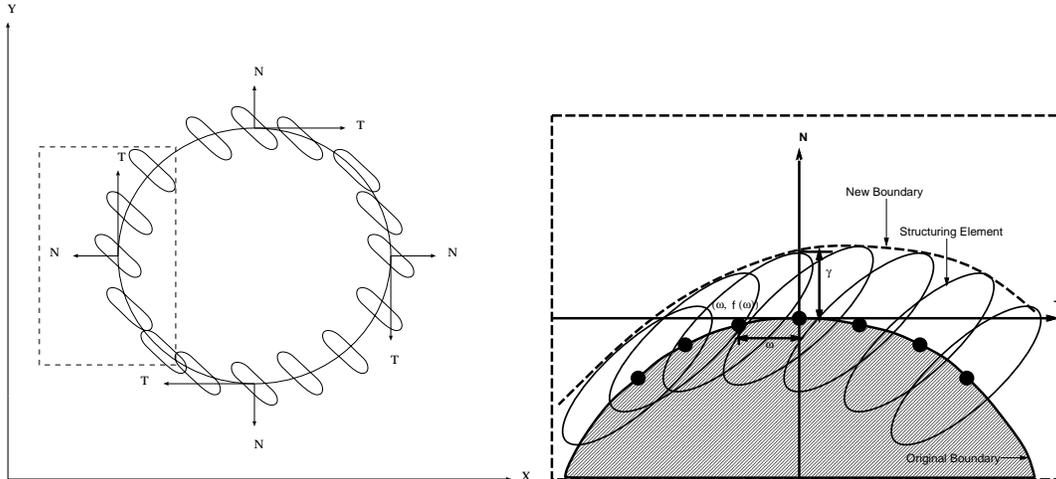
Figure 2: Morphological operations in the extrinsic and intrinsic coordinates for an arbitrary convex structuring element.

reparametrization is employed, but this is at the expense of smoothing singularities, the salient features of shape. Finally, numerical simulations of boundaries are prone to a buildup of discretization error.

To effectively deal with these problems, we embed the original evolution equation in a higher dimension. This is achieved by representing the evolving curve as the zero level set of an evolving surface. Observe that the evolving surface can handle topological events and since the grid is fixed, no resampling is needed. There are more subtle arguments for re-posing the curve evolution problem as a surface evolution problem; for more details see [13, 11].

Formally, let $z = \phi_0(x, y)$ denote the initial surface, which is obtained from the initial curve by placing a "tent" on it, e.g., its distance transform [22]. If the evolving surface, $z = \phi(x, y, t)$, satisfies

$$\begin{cases} \phi_t + \beta(\phi_x^2 + \phi_y^2)^{1/2} = 0 \\ \phi(x, y, 0) = \phi_0(x, y), \end{cases} \quad (19)$$

then its zero level set evolves according to (4), [13]. Since we have already shown that $\beta = \beta(\theta(s, t))$ and since

$$(\cos\theta, \sin\theta) = \frac{(-\phi_y, \phi_x)}{\sqrt{\phi_x^2 + \phi_y^2}}, \quad (20)$$

it is clear that β is a function of ϕ_x and ϕ_y, namely, only the first derivatives of ϕ. Therefore, equation (19) can be rewritten as

$$\begin{cases} \phi_t + \mathcal{H}(\phi_x, \phi_y) = 0 \\ \phi(x, y, 0) = \phi_0(x, y), \end{cases} \quad (21)$$

where $\mathcal{H}(\phi_x, \phi_y) = \beta(\phi_x, \phi_y)(\phi_x^2 + \phi_y^2)^{1/2}$ is the Hamiltonian associated with this Hamilton-Jacobi equation. These equations are of paramount significance in the physical sciences, also referred to as the canonical, or

the eikonal equation. A number of computer-vision problems can be modeled using Hamilton-Jacobi equations [13, 12, 14, 16, 23].

Numerical Implementation In addition to theoretical implications, theorem 1 when written as (21), leads to a robust, highly accurate numerical method for the implementation of morphological transforms. While fast, accurate methods for implementing mathematical morphology have been previously devised, these methods are for a restricted class of structuring elements. In addition iterating mathematical morphology operations for certain structuring elements leads to numerical inaccuracy. In contrast, our method implements an efficient discrete iteration of arbitrary convex morphological transformations that are currently not realizable via existing methods.

A variety of algorithmic methods have been proposed in literature to implement morphological transformations [32]. These include: parallel algorithms, sequential algorithms [21], algorithms based on queues [32], loops [26], quadtrees [24], run-length encoding [19], etc. Although at least two classes of algorithms (queues and loops) are well suited to implementing successive dilations with (small) structuring elements, Figure 3, none of these methods can deal with structuring elements which are not digitally scalable:

Definition 1 Let $\mathcal{B}$ denote a convex compact set of $\mathbb{R}^2$ and $d(\mathcal{B})$ denotes its $\mathbf{Z}^2$ digitization: $d(\mathcal{B}) = \mathcal{B} \cap \mathbf{Z}^2$. We say that $\mathcal{B}$ is DIGITALLY SCALABLE if and only if

$$\forall n \geq 1, d(n\mathcal{B}) = nd(\mathcal{B}), \quad (22)$$

where,

$$n\mathcal{B} = \underbrace{\mathcal{B} \oplus \mathcal{B} \oplus \cdots \oplus \mathcal{B}}_{n \text{ times}}.$$
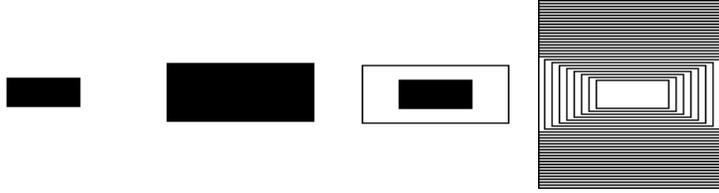
Figure 3: This figure illustrates the dilation of a rectangle by a structuring element of the same shape, implemented using the algorithm presented in [31]. Left to right: the original rectangle; theoretically expected rectangle; the rectangle dilated in a single step and superimposed on the original; the rectangle dilated iteratively. The results for the rectangle are indeed accurate, as the rectangle is digitally-scalable.

Typically, a square or a rectangle structuring element is scalable, but an ellipse or a disk is not. As Figure 4 illustrates, iterated dilations of a structuring element in the discrete domain may not yield a single dilation with a larger structuring element as in the continuous domain. It appears that the scalability of structuring elements does not carry over to the discrete domain for all structuring elements. While algorithms have indeed been published to compute Euclidean distance functions [3, 30, 18, 15], from which successive dilations by disks can be derived by simple thresholding, more complex convex non digitally scalable elements are intractable.

In contrast, the numerical simulation of the Hamilton-Jacobi equation (21) deals with such structuring elements and is not amenable to such discrete errors. Figure 5 illustrates the iterated dilations of an ellipse with an infinitesimal elliptical structuring element of the same shape. As expected, the dilations at any step in the iteration represent an ellipse and the boundaries are represented highly accurately. Our algorithm is best suited for applications where incremental morphology is necessary, or where the dynamics of dilations/erosions is of interest. In general, it handles topological merging and splitting as well, making it possible to detect when, *e.g.*, some connected components have merged. For a more detailed description of these simulations see [1, 13, 11].

References

[1] A. Arehart, L. Vincent, and B. B. Kimia. Mathematical morphology: The Hamilton-Jacobi connection. Technical Report LEMS 108, Brown University, June 1992.

[2] R. Brockett and P. Maragos. Evolution equations for continuous-sacle morphology. In *Proceedings of the IEEE Conference on Acoustics, Speech and Signal Processing*, San Francisco, CA, March 1992.

[3] P. Danielsson. Euclidean distance mapping. *Computer Graphics and Image Processing*, 14:227–248, 1980.

[4] R. V. den Boomgaard. Mathematical morphology: extensions towards computer vision. Ph.D. dissertation, University of Amsterdam, March 1992.

[5] R. M. Haralick, S. R. Sternberg, and X. Zhuang. Image analysis using mathematical morphology. *PAMI*, 9(4):532–550, July 1987.

[6] H. Heijmans. Theoretical aspects of gray-level morphology. *IEEE Transactions on Pattern Analysis and Machine Intelligence*, 13:568–582, 1991.

[7] F. John. *Partial Differential Equations*. Springer-Verlag, 1971.

[8] B. B. Kimia, A. R. Tannenbaum, and S. W. Zucker. Toward a computational theory of shape: An overview. CIM-89-13, McGill Centre for Intelligent Machines, McGill University, Montreal, Canada, 1989.

[9] B. B. Kimia, A. R. Tannenbaum, and S. W. Zucker. Toward a computational theory of shape: An overview. In O. Faugeras, editor, *Lecture Notes in Computer Sceience, 427*, pages 402–407, Berlin, 1990. Springer Verlag.

[10] B. B. Kimia, A. R. Tannenbaum, and S. W. Zucker. Entropy scale-space. In C. Arcelli, editor, *Visual Form: Analysis and Recognition*, pages 333–344, New York, May 1991. Plenum Press.

[11] B. B. Kimia, A. R. Tannenbaum, and S. W. Zucker. On the numerical implementation of shape evolution. *In Preparation*, 1992.

[12] B. B. Kimia, A. R. Tannenbaum, and S. W. Zucker. On the role of generalized function theory in computer vision. *In Preparation*, 1992.

[13] B. B. Kimia, A. R. Tannenbaum, and S. W. Zucker. Shapes, shocks, and deformations, I: The components of shape and the reaction-diffusion space. *International Journal of Computer Vision*, Submitted, 1992.

[14] R. Kimmel, K. Siddiqi, B. B. Kimia, and A. Bruckstein. Shape from shading via level sets. *International Journal of Computer Vision*, Submitted, 1992.
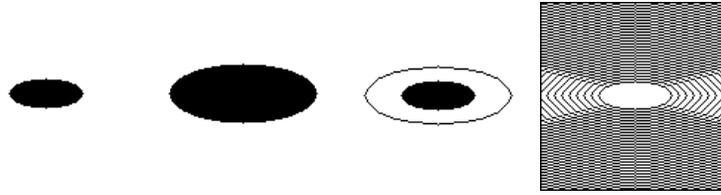
Figure 4: This figure illustrates the dilation of an ellipse by a structuring element of the same shape, implemented using the algorithm presented in [31]. Left to right: the original ellipse; theoretically expected ellipse; the ellipse dilated by in a single step and superimposed on the original; the ellipse dilated iteratively. Note that while the results when dilation is implemented in a single step are highly accurate, the iterations of a small structuring element in this case do not produce desirable results, as the ellipse is *not* digitally-scalable.
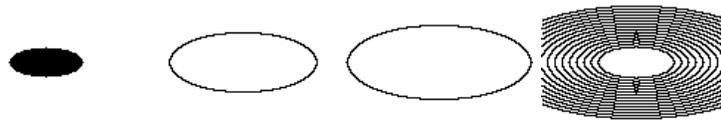

Figure 5: An illustration of the numerical simulation of the Hamilton-Jacobi equation (19). Left to right) the original ellipse; the ellipse dilated by 100 steps; the ellipse dilated by 150 steps; samples of the iterations superimposed on the same image. Note that the shape of the ellipse remains elliptical, as expected. The results are highly accurate and robust.

[15] F. Leymarie and M. D. Levine. Fast raster scan distance propagation on the discrete rectangular lattice. 55(1):84–94, Jan. 1992.

[16] F. Leymarie and M. D. Levine. Simulating the grassfire transform using an active contour model. 14(1):56–75, Jan. 1992.

[17] G. Matheron. *Random Sets and Integral Geometry*. Wiley, 1975.

[18] D. Paglerioni. Distance transforms: Properties and machine vision applications. *CVGIP: Graphical Models and Image Processing*, 54(1):56–74, January 1992.

[19] L. Piper and J.-Y. Tang. Erosion and dilation of binary images by arbitrary structuring elements using interval coding. *Pattern Recognition Letters*, pages 201–209, April 1989.

[20] J. Roerdink. Manifold shape: from differential geometry to mathematical morphology. In *Proceedings NATO Shape in Picture Workshop*, number 4, Driebergen, NL, September 1992.

[21] A. Rosenfeld and J. Pfaltz. Sequential operations in digital picture processing. *J. Assoc. Comp. Mach.*, 13(4):471–494, 1966.

[22] A. Rosenfeld and J. Pfaltz. Distance functions on digital pictures. *Pattern Recognition*, 1:33–61, 1968.

[23] E. Rouy and A. Tourin. A viscosity solutions approach to shape-from-shading. *SIAM. J. Numer. Analy.*, 29(3):867–884, June 1992.

[24] H. Samet. The quadtree and other related hierarchical data structures. *ACM Computing Surveys*, 16(2):87–260, 1984.

[25] G. Sapiro, B. B. Kimia, , R. Kimmel, D. Shaked, and A. Bruckstein. Implementing continuous-scale morphology. *Pattern Recognition*, In Press, 1992.

[26] M. Schmitt. Des algorithmes morphologiques à l'intelligence artificielle. Ph.D. dissertation, Ecole des Mines, Paris, France, February 1989.

[27] J. Serra, editor. *Image Analysis and Mathematical Morpholpogy*. Academic Press, 1982.

[28] J. Serra, editor. *Image Analysis and Mathematical Morpholpogy, Part II: Theoretical Advances*. Academic Press, 1988.

[29] L. Vincent. Graphs and mathematical morphology. *Signal Processing*, 16(4):365–388, April 1989.

[30] L. Vincent. Exact euclidean distance function by chain propagations. In *Proceedings of the IEEE Computer Vision and Pattern Recognition '91*, pages 520–525, Maui HI, 1991.

[31] L. Vincent. Morphological transformations of binary images with arbitrary structuring elements. *Signal Processing*, 22(1):3–23, 1991.

[32] L. Vincent. *Morphological algorithms*, pages 255–288. Marcel-Dekker, September 1992.